Thermal and hydrodynamic performance of a microchannel heat sink with carbon nanotubes nanofluids: Effect of concentration and channel section

Normah Mohd-Ghazali, Patrice Estellé, Salma Halelfadl, Thierry Maré, Tng Choon Siong, Ummikalsom Abidin

Thermal and hydrodynamic performance of a microchannel heat sink with carbon nanotubes nanofluids: Effect of concentration and channel section

Normah Mohd-Ghazali[a], Patrice Estellé[b,*], Salma Halelfadl[b], Thierry Maré[b], Tng Choon Siong[a], Ummikalsom Abidin[a]

[a] Faculty of Mechanical Engineering, Universiti Teknologi Malaysia, Skudai, 81310 Johor Bahru, Malaysia

[b] Univ Rennes, LGCGM, EA 3913, 35000 Rennes, France

* Corresponding author: patrice.estelle@univ-rennes1.fr

Highlights

- Comparison of optimized thermal and hydrodynamic performances of a circular and square microchannel heat sink cooled with carbon nanotube nanofluid, using experimentally obtained data.
- Analysis of surfactant and viscosity effects on CNT nanofluid performance.
- Utilization of multi-objective genetic algorithm (MOGA) to simultaneously minimize the thermal resistance and pressure drop.

ABSTRACT

Increasing heat fluxes in decreasing sizes of a microchannel heat sink have necessitated studies into better systems, in particular a more capable coolant for improved thermal management. Nanofluids have been at the forefront with their higher thermal conductivity as compared to the base fluid alone. However, few investigations have looked into the role played by surfactants, a component used for dispersion and stability of nanofluids, and their influence on thermophysical properties and thermal performance. Optimized performances of carbon nanotube nanofluids with different surfactants at different volume fraction under laminar flow are studied. Using the thermal resistance model and experimental data for thermal conductivity and viscosity of nanofluids, the thermal resistance and pumping power are simultaneously minimized using multi-objective genetic algorithm. Results showed that the nanotube nanofluid with lignin as the surfactant performed better thermally and hydrodynamically, due to lower viscosity at high carbon nanotubes concentration compared to the nanotube nanofluid with sodium polycarboxylate surfactant. As an example, a 29% and 28% increase in pressure drop is found for sodium polycarboxylate based nanofluid at a volume fraction of 0.1% for a circular and square MCHS respectively. A similar pattern is observed at higher volume fraction as

well, even higher pressure drop with increasing volume fraction. Also, it is shown that microchannel heat sink with circular cross section performed better than with square section.

Keywords: *Microchannel heat sink; Optimized; Nanofluids; Surfactant; Carbon nanotube; Genetic algorithm*

1. Introduction

As microelectronics devices design continue towards miniaturization and becoming more complex, the power density is increasing with effective cooling of the active components needed to ensure their optimum operation. Sensitive components such as integrated circuits, which are the main generators of heat, are vulnerable to temporary or permanent failure if overheated. Thus, the landmark study by Tuckerman and Pease in 1981 [1] of using a microchannel heat sink (MCHS) in very large-scale integration (VLSI) circuits have attracted great interests from many researchers due to its proven effective and compact heat removal from a small area.

Efforts into the enhancement of the cooling capacity of a MCHS have much focussed on the structural materials [2-7], different channel shapes [8-11], effect of entrance channel shapes [12] and various types of coolants [1, 2, 13-15]. To date, it seems that research into the structural material and common channel geometries have almost reached its saturation stage [16]. However, the introduction of fins within the channels can lead to heat transfer improvement as shown in [17]. This numerical analysis based on optimization procedure demonstrated that heat transfer of water in laminar regime within microchannel heat sink with pin-fin and dimple is enhanced with both the increase in pin diameter and the reduction in stream-wise spacing. The effect of triangular cavities and rectangular ribs on heat transfer performance of microchannel heat sink under laminar regime was also investigated numerically in [18]. These authors evidenced uniform and lower temperature at the substrate of the heat sink and reported better heat transfer performance with cavities and ribs than without. They also proposed the better combination of cavities and ribs to achieve higher performance. Moreover, thermal performance of air-cooled heat sink was obtained from simulation by Moradikazerouni et al. [19] who also studied spatial variation of plate fins in forced convection flow. Vinoth and Senthil Kumar [20] demonstrated from experiments that trapezoidal cross-section oblique finned micro-channel appear to be more suitable for heat transfer enhancement than square and

semicircle cross section. In addition, Al_2O_3/water nanofluid of volume fraction 0.25% also increase heat transfer in comparison to water. Convective heat transfer and pressure drop of microchannel heat sink with multiple zigzag flow channels were experimentally studied by Duanthongsuk and Wongwises considering SiO_2 -water nanofluids [21]. They compared the performance of a continuous zigzag flow channel and a zigzag flow channel with a single cross-cutting at the middle position. An higher Nusselt number was obtained with nanofluids compared to water while better heat transfer performance was obtained with the presence of single cross-cutting. Few time ago, the fluid flow and heat transfer of γ-AlOOH-50/50 water-ethylene glycol nanofluid flowing through a sinusoidal wavy channel was investigated by Vo et al. [22] showing also the influence of nanoparticles shape in heat transfer performance.

Moreover, improvement of heat transfer capabilities with variations in the thermophysical properties of fluids have been continuously of interest. The thermal conductivity and heat capacity - two properties responsible towards a coolant ability to remove heat - of air, water, and refrigerants could be manipulated through the addition of moisture in the case of gas, and particles for the liquids. The latter has become the trending coolant with continuous studies into different particles with various concentrations dispersed in various base fluids [23,24,25]. The enhanced heat transfer attainable with nanofluids have made them as a popular choice of coolants [26], as also evidenced in some of the previous references.

Unlike the standard nanofluids with spherical oxide or metallic particles immersed in based fluid, fewer studies have been completed on the use of carbon nanotubes (CNT) based nanofluids in microchannel heat-sink. Recently, Arani et al. [27] numerically investigated heat transfer rate of CNT nanofluids flowing through a truncated double-layered microchannel heat sink. From theoretical models for nanofluid properties, they showed the increase in heat transfer with nanoparticle content and the reduction in thermal resistance with the increase in Re or nanoparticle loading. An experimental investigation on thermal performance and fouling of CNT/water nanofluid inside a heat sink with rectangular microchannel was performed by Sarafraz et al. [28]. Temperature profile along the channel length was reported to decrease with nanoparticle content that also lead to the increase in heat transfer compared to water. Lastly, the laminar heat transfer of kerosene nanofluid/multi-walled carbon nanotubes in the microchannel heat sink was numerically studied by Arabpour et al. [29]. Increasing Reynolds number and volume fraction of nanoparticles produced the increase in convection heat transfer that reduced the maximum temperature. The reduction in thermal resistance that causes the enhancement of heat transfer amount was also reported to be dependant of slip velocity at walls.

Different results have been reported in the literature [30-32] on the analytical models of the thermophysical properties on CNT. Thus, only experimentally obtained properties of the CNT nanofluid, specifically for thermal conductivity and viscosity, have to be preferably used in modelling of its performance in any cooling system as reported by Halelfadl et al. [15] and Nik Mazlam et al. [233]. It has been established that dispersion and stability of the nanoparticles can be prevented with the addition of surfactant though their specific effects have hardly been studied. As reported earlier in laminar pipe flow [34], experimentally obtained thermophysical properties of CNT nanofluids are here used to determine the optimized thermal and hydrodynamic performance of a MCHS. Two types of CNT nanofluids are investigated and mainly differs in types of surfactants used, lignin and sodium polycarboxylate, respectively.

Although circular geometry is better in terms of fluid flow due to the absence of corners, fabrication of a circular MCHS has been an issue till late. Advances in the manufacturing technology could make it feasible and advantageous in heat transfer considering the physics of the flow. Thus, the objective of this study is also to compare the performance of circular and square geometry through simultaneous minimization of the thermal resistance and pumping power of a MCHS cooled with CNT nanofluids. The thermal resistance model is utilized with multi-objective optimization algorithm (MOGA), a search tool the authors found to be capable of a global search in the presence of multiple conflicting objectives [11, 12, 15, 24, 33]. It has been known that the pressure drop tends to increase with the increase in the thermal resistance of a MCHS, MOGA has been used by the authors in their previous studies with a MCHS. The model developed by Ghazali-Mohd et al. [11] is used here to look into how different surfactant affecting the thermophysical properties of CNT nanofluids contributes on the thermal and hydrodynamic performance of a CNT nanofluid-cooled MCHS.

2. Mathematical modeling

A schematic structure of the aluminium circular and square MCHS used is shown in Fig. 1 [11]. The MCHS has the dimension $L \times W$ of 1×1 cm with a height of 0.213 mm. The size is based on previous studies [1,15]. A series of parallel channels run the length of the MCHS.

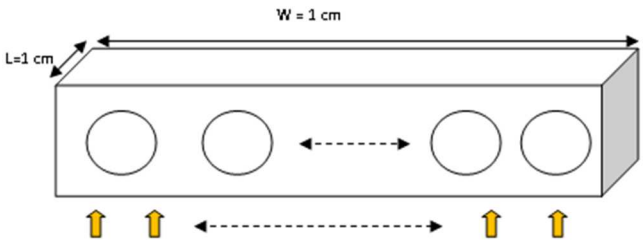

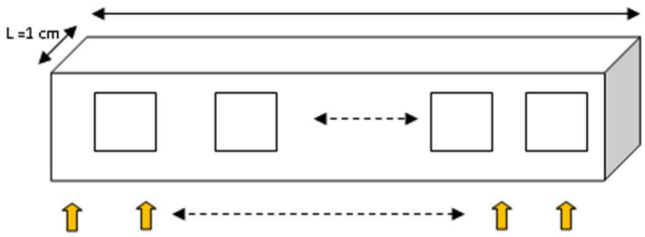

Figure 1. Microchannels considered in the study.

Each microchannel has a hydraulic diameter, H_c. A uniform constant heat flux is assumed to be applied from the bottom of the MCHS which is connected to the electronics chip. Working fluid at the flow rate of $G = 4.7\times10^{-6}$ m^3/s enters the series of parallel channels along the length of the MCHS to remove the heat flux generated. On top of the MCHS, it is covered by an adiabatic cover plate. The entire chip area can be cooled by this system. The dimensions of the MCHS are given in Table 1.

Table 1. Geometrical properties of the model [11]

Length, $L(m)$	0.01
Width, $W\,(m)$	0.01
Substrate thickness, $t\,(m)$	213×10^{-6}
Thermal conductivity, $k\,(W/m{\cdot}K)$	238

The total thermal resistance is contributed by the substrate below the channels, R_{cond}, the convective heat transfer, R_{conv}, and the coolant heat capacity, R_{cap}, where the resistances are assumed to be in series. In the optimization process of the MCHS, H_c and the ratio of the wall width, W_w, to H_c are the variables to be optimized to achieve simultaneous minimization of the thermal resistance and pumping power. The total thermal resistance according to the thermal resistance model can be determined from,

$$R_{total} = \frac{t}{k_s(LW)} + \frac{L}{c_{pf}\mu_f Re} \times \frac{1+\beta}{WL} \times j_{cap} + \frac{H_c}{k_f Nu} \times \frac{1+\beta}{WL} \times j_{conv} \qquad (1)$$

where j_{conv} takes the value of 1/3 and $1/\pi$, for the square and circular MCHS respectively, while j_{cap} takes the value of unity and $4/\pi$ for the square and circular MCHS respectively. The hydraulic diameter, H_c, and channel wall width to channel width ratio, β, are regarded as variables,

$$\beta = \frac{W_w}{H_c} \qquad (2)$$

Similar to the thermal resistance, the hydraulic resistance is represented by the total pressure drop used in [11]:

$$\Delta P = m \frac{LG}{W} \frac{\mu_f}{H_c^2} (1 + \beta) \qquad (3)$$

In this investigation of the effect of surfactants on thermphysical properties and heat transfer performance of nanofluids flowing in MCHS, m for the circular and square channels used are $\frac{128}{\pi H_c}$ and $\frac{57}{2H_c}$, respectively. Equation (1) and equation (3) have conflicting effects. Both are desired to be as low as possible but the lowering of Equation (1) results in an increase in equation (3), and vice versa. Thus, simultaneous minimization of both functions is sought. This can be achieved with MOGA [11].

3. Optimization with MOGA

Generally, optimization problems consist in discovering the best solution from all feasible solutions. The optimization procedure applied here is based on past studies [11], [12], [14], mathematically represented as,

$$min \bar{f}(\bar{x}) = \left[f_{1(\bar{x})}, f_{2(\bar{x})}, \dots, f_{\mathrm{m}(\bar{x})} \right] \qquad (4)$$

for m = 1, 2, …, M for the number of objective functions, in this study M = 3. Meanwhile, $\bar{x}$ is a vector containing the design variables which in this case are H_c and β.

The optimization solver of multi-objective optimization using Genetic Algorithm is chosen as the current problem exhibited a multi-objective nature. The two objective functions to be minimized are selected to describe the overall performance of the microchannel heat sink. The first objective function is associated with the thermal performance that is the total thermal resistance, Equation (1), while the second is related to the hydrodynamic performance that is the pressure drop, Equation (3). Next, the bounds are created for the design variables. Two design variables used in the optimization procedure include the hydraulic diameter, H_c, and channel wall width to channel width ratio, β, with their lower and upper bounds limit specified in Table 2, based on past studies.

Table 2. Design variables limits

Design variables	Lower Limits	Upper limits
H_c	0.0005	0.003
β	0.1	0.2

In the optimization process of a MCHS, H_c, and β were regarded as variables while the other parameters were fixed. After that, the optimization options such as population, selection, reproduction, mutation, crossover, migration and stopping criteria were also set in order to generate a Pareto optimal front for both objective functions. Several solutions were also generated to determine the most appropriate combinations of the optimization options. Those options are specified in Table 3.

Table 3. Optimization options set for the current study

Population size	120
Selection function	Tournament
Crossover fraction	0.8
Mutation function	Constraint Dependent
Crossover function	Intermediate
Migration direction	Forward
Stopping criteria (function tolerance)	1×10^{-4}

Lastly, Fig. 2 describes the complete optimization procedure employed in the current research.

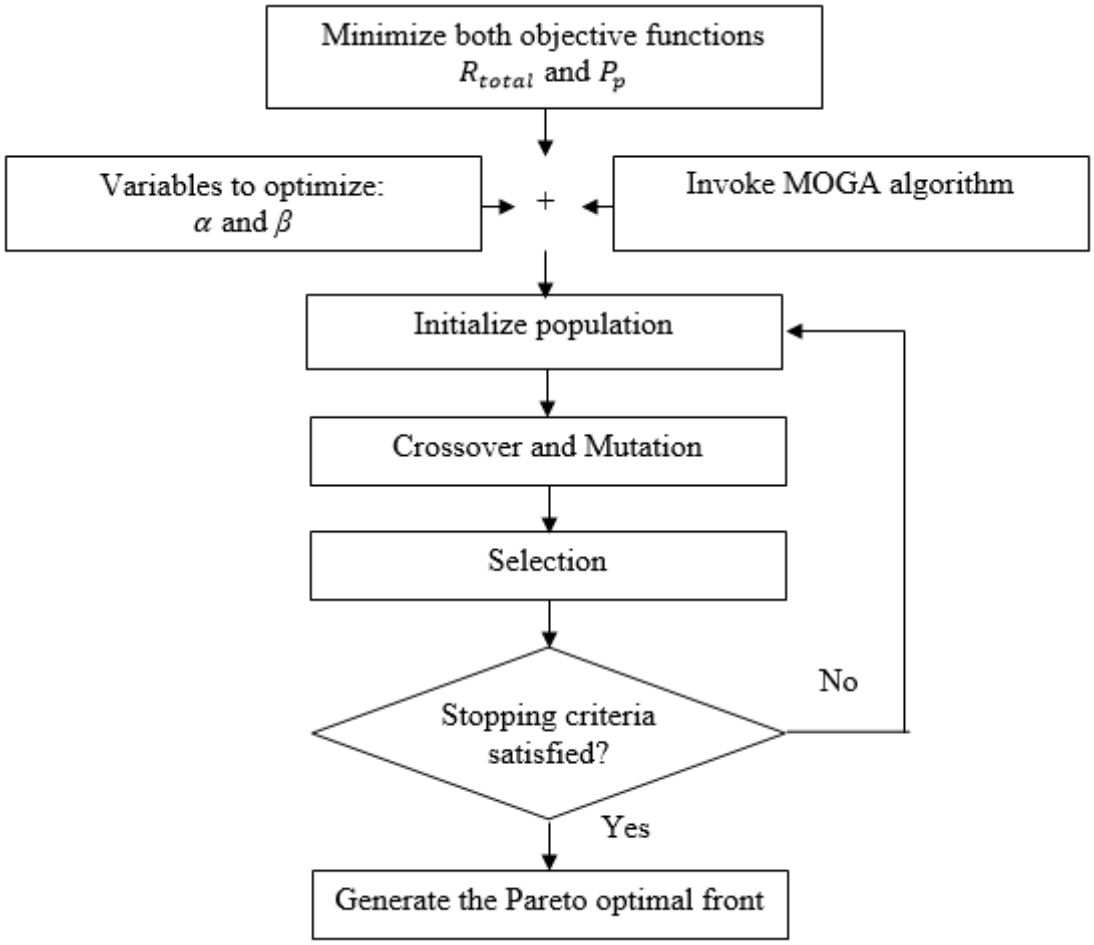

Figure 2. Optimization procedure (adapted from [14])

4. Carbon Nanotube Nanofluids

The water based-CNT nanofluids presently considered were previously investigated [35]. In short, they consisted in carbon nanotubes (density 1800 kg/m^3 ; purity 90%) of 9.2 nm and 1.5 μm in average diameter and length respectively, dispersed in a mixture of water and surfactant. It is noted that the weight ratio between surfactant and nanoparticle content was kept constant for each studied concentration in nanotubes. Two types of surfactant were considered namely lignin and sodium polycarboxylate. They were used to improve the dispersion and stability of CNT within water and reduce clogging and sedimentation with time. Their preparation and the evaluation of their thermophysical properties at 20°C were reported earlier for volume fraction ranging from 0.0055% to 0.55%. In brief, density and heat capacity were obtained from mixing rules using equations developed by Pak and Cho [36] and O'Hanley et al. [37] respectively as described in [38]. Thermal conductivity and viscosity were experimentally determined from well-designed procedures in [35,39,40]. All these results are

shown in Figure 3. In the following, nanofluids produced with lignin are labelled N_2. N_3 is used for nanofluids obtained with sodium polycarboxylate as surfactant.

So, Figure 3 shows that density and heat capacity of nanofluids increases, respectively decreases, with volume fraction as generally reported in literature. In addition, both properties are similar for both nanofluids. Regarding the thermal conductivity of nanofluids, it obviously increases with nanoparticle content with similar trend and values for both nanofluids. While the type of surfactant used in the CNT nanofluid preparation has no effect on the previous thermophysical properties, a difference is observed for viscosity. The effect is graphically represented in Figure 3 where, as the volume fraction increases just beyond 0.03%, the viscosity for N_2 and N_3 diverged in value, N_3 being highly affected with a sharp increase in viscosity up to 0.55%.

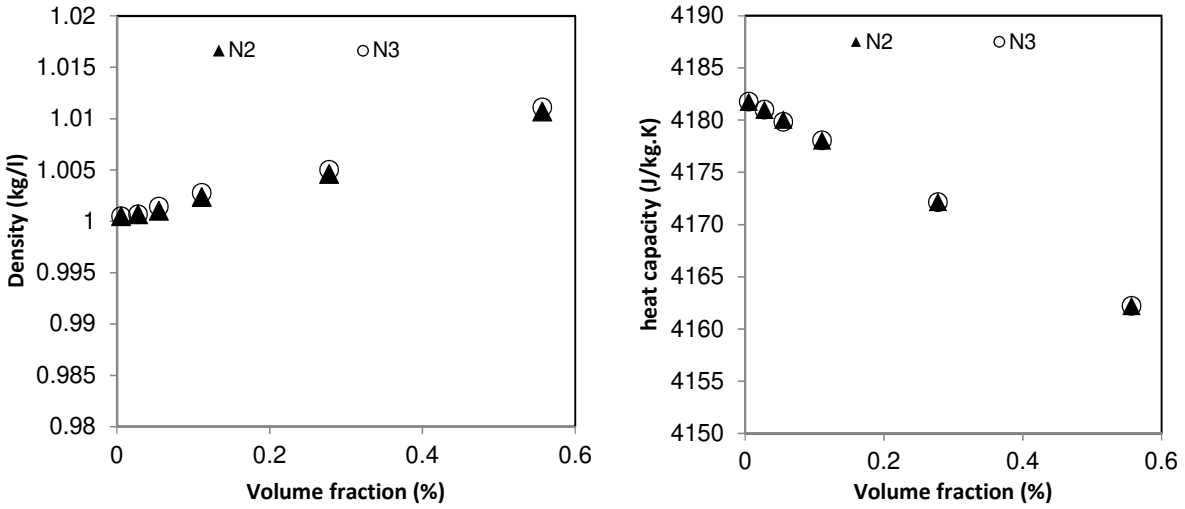

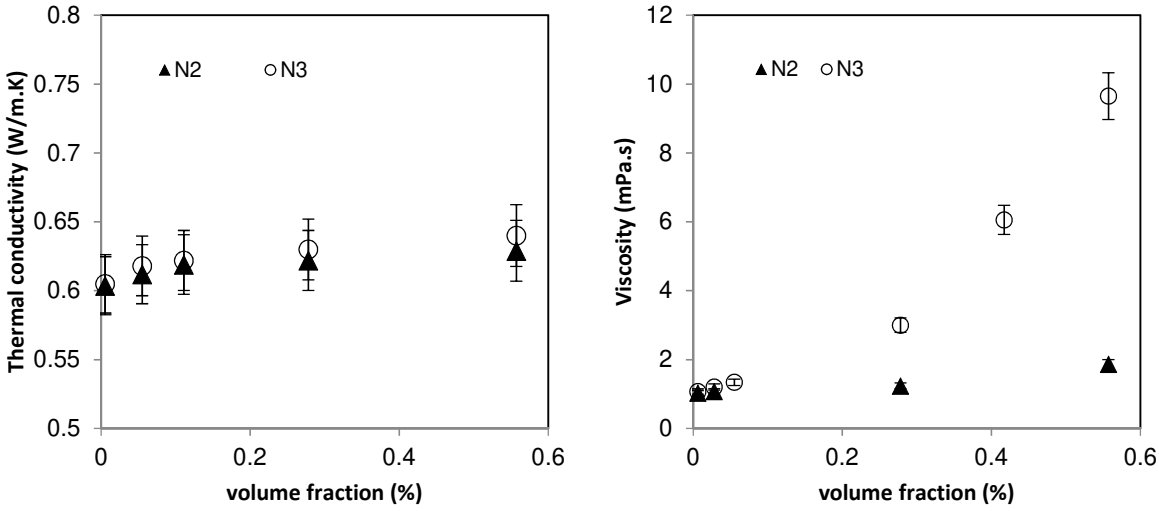

Figure 3. Thermophysical properties of CNT nanofluids at 20°C – effect of CNT concentration and surfactant

These graphs already indicate the necessity to appraise the types of surfactant used and its effect on the desired properties looked for, the thermal and hydrodynamic performances. They also show the interest of using experimental data rather than models that could not be relevant for nanofluids.

All thermophysical properties at 20°C are modeled through the experimental data reported in Figure 3 in order to make easier their use for the optimization procedure. These equations are presented in Table 5. Based on previous observations, similar equations were used with both nanofluids for density, heat capacity and thermal conductivity.

Table 5. Models for the thermophysical properties of CNT nanofluids.

$k\ (W/m.K)$	y = 0.0072ln(x) + 0.6405
$\rho(kg/m^3)$	y = 0.0019x + 1.0011
$C_p(J/kg.K)$	y = -36.794x + 4178.7
$\mu\ (mPa.s)$	y = 2.7933x^2 - 0.0924x + 1.0539 (N_2) y = 28.98x^2 - 0.8218x + 1.1761 (N_3)

5. Results and discussion

The effects of the particle volume fraction on the thermal resistance and pressure drop is presented first for N_2 in a circular MCHS, for the volume fractions of 0.1%, 0.2%, 0.3%, and 0.5% at 20°C. The pattern and trend exhibited are expected for the thermal and hydrodynamic performance of a MCHS where a decrease in the thermal resistance is followed by an increase in the pressure drop as shown in Fig. 4.

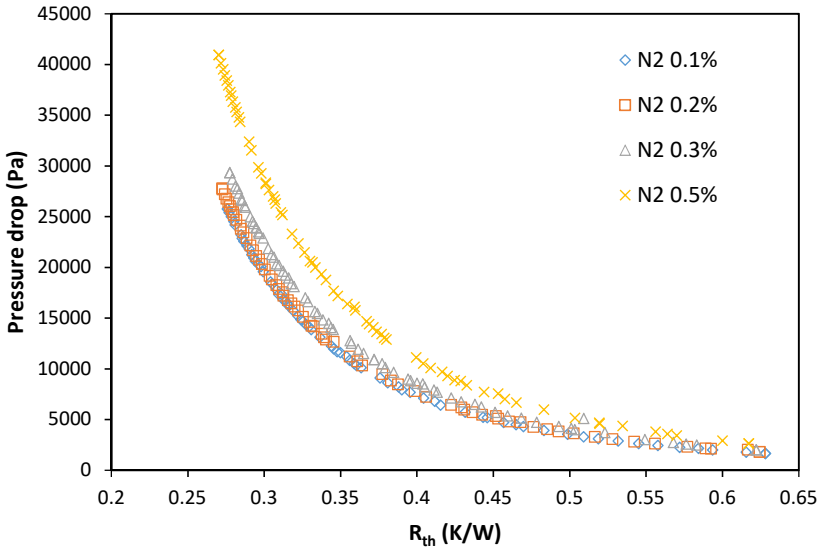

Figure 4. Pressure drop and thermal resistance of a circular MCHS at various volume fractions.

Up to 0.3%, the difference between the volume fractions does not seem to affect much on the performance of the MCHS. A previous study [8] showed that the increased nanoparticles volume fraction increased the thermal conductivity of the coolant as well as increased the convective heat transfer coefficient which in turn reduces the convective thermal resistance. Since both N_2 and N_3 nanofluids have the same nanotubes and thermophysical properties except for the viscosity, a similar trend is expected with their thermal and hydrodynamic performances. Thus, a comparison of the performance in a circular and square MCHS is presented next in Fig. 5, Fig. 6 and Fig. 7 for the volume fraction of 0.1%, 0.3% and 0.5% respectively. For each case of a circular or square MCHS, at any particular thermal resistance, R_{th}, the pressure drop is higher for N_3 than for N_2, showing the effect of the surfactant used and its influence on dispersion state of nanotubes and viscosity increase. For a circular MCHS at 0.63 K/W, the pressure drop for N_3 is 21% higher than that for N_2, while for the square MCHS at 0.63 K/W,

the pressure drop for N_3 is 28% higher than that for N_2. Hence, N_2 nanofluid is more preferable if a lower pumping power is desirable for the same thermal performance. The difference in the performance becomes more significant as the volume fraction increases as seen in Fig. 6 and Fig. 7. The pressure drop also increases as the volume fraction is increased at any thermal resistance.

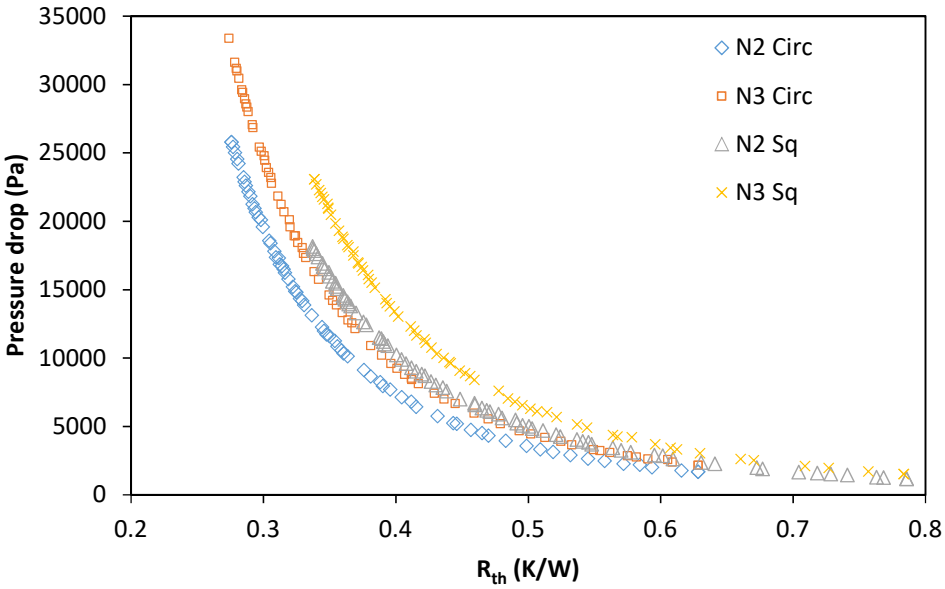

Figure 5. Comparison of the pressure drop and thermal resistance of the circular and square MCHS at 0.1%.

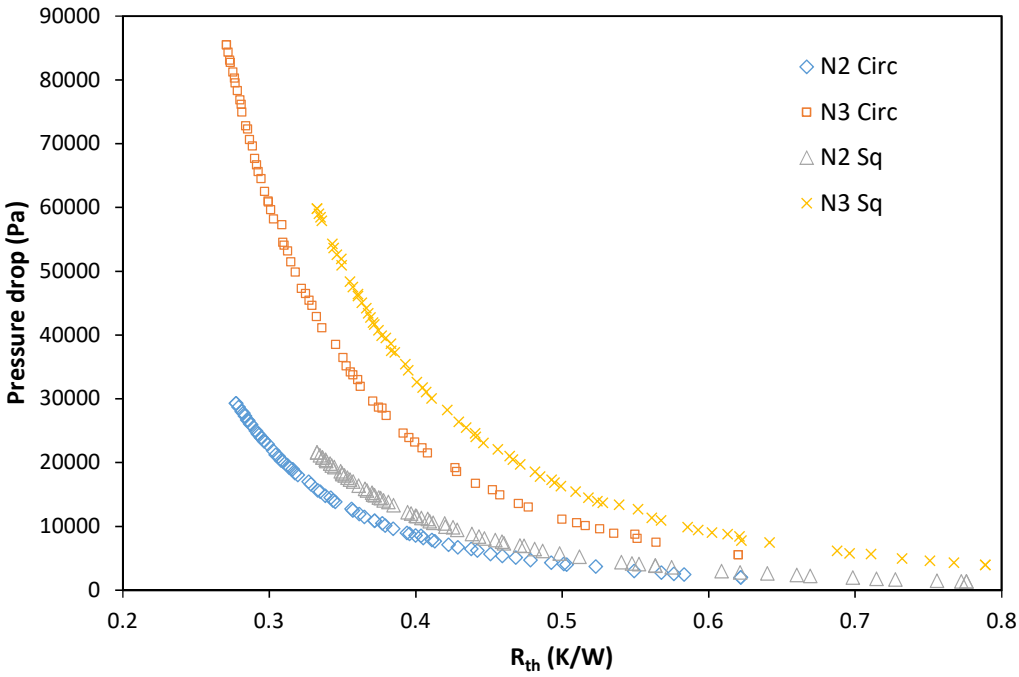

Figure 6. Comparison of the pressure drop and thermal resistance of the circular and square MCHS at 0.3%.

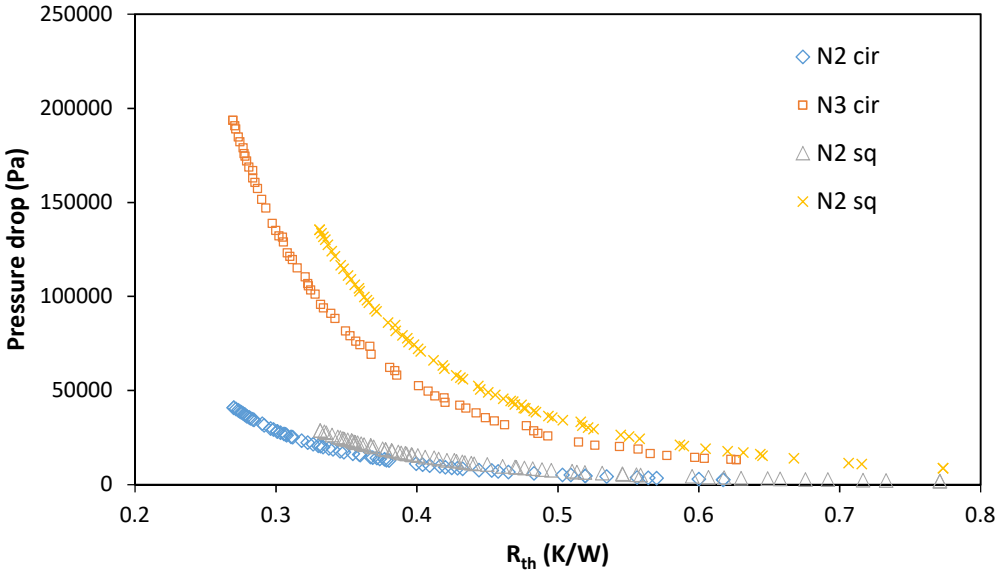

Figure 7. Comparison of the pressure drop and thermal resistance of the circular and square MCHS at 0.5%.

Fig. 8 and Fig. 9 show the effect on the pressure drop as the hydraulic diameter of the channel increases, for the case of 0.1% and 0.5% volume fraction, respectively.

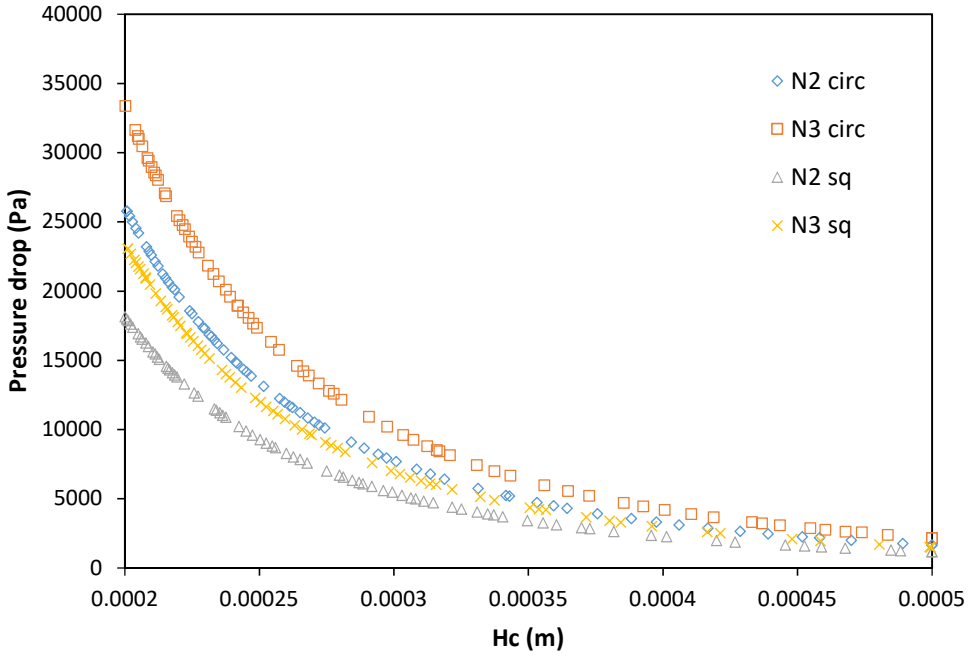

Figure 8. Effect of hydraulic diameter on the pressure drop of the circular and square MCHS at 0.1%.

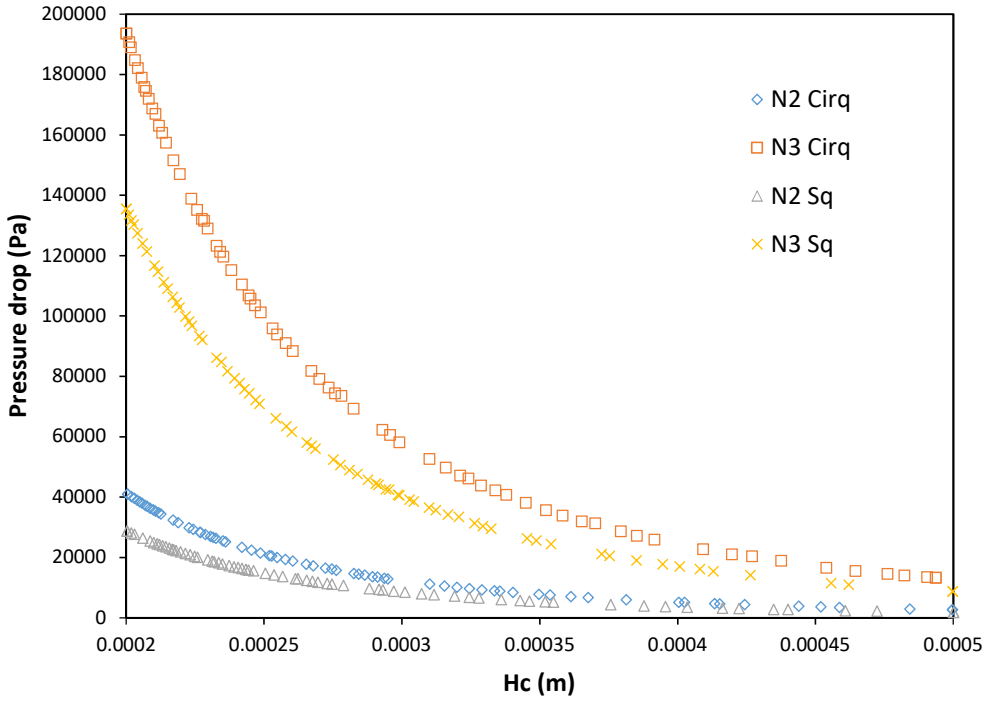

Figure 9. Effect of hydraulic diameter on the pressure drop of the circular and square MCHS at 0.5%.

As the hydraulic diameter increases, the expected decrease in pressure drop is observed. N_3, however, showed a significant increase in the pressure drop which subsequently will result in a higher pumping power for the heat sink to operate with the coolant. The type of surfactant used has no effect on the thermal performance as listed in Table 6 for 0.1% volume fraction, selected at the hydraulic diameter of 201 mm. The wall width, W_w, and number of microchannels, n, in each MCHS are also listed in Table 6. An increase of 29% and 28% in pressure drop is expected when N_3 is used instead of N_2, for a circular and square MCHS respectively.

Table 6. Pressure drop (DelP) and pumping power (Pp) at the lowest thermal resistance, 0.1%.

	Hc (µm)	Rth (K/W)	DelP (kPa)	Pp (W)	β	W_w (β×Hc) (µm)	n
N2C (0.1%)	201	0.27	25.8	0.121	0.0154	3.1	49
N3C (0.1%)		0.27	33.4	0.157	0.0101	2.03	49
N2S (0.1%)		0.34	18.0	0.085	0.0106	2.13	49
N3S (0.1%)		0.34	23.1	0.109	0.0115	2.31	49

For the same channel height and number of channels per MCHS, the thermal performance is the same for N_2 and N_3 but hydrodynamically, N_2 outperformed N_3 because of the change in

viscosity. This applies for both the circular and square geometries. The higher pumping power required for the circular MCHS is due to the smaller cross-sectional area involved, 20% smaller than that of the square geometry. The same effect is observed at other volume fractions. With a lower thermal resistance at a higher pumping power, flow in circular channels eliminates the potential secondary flow that could occur in the square MCHS. The phenomenon could reduce the effectiveness of the channel wall and consequently affect the thermal performance of the MCHS.

Finally, the outcomes of this study showed that serious consideration is needed with the selection of surfactant when energy use is an issue. Actually, while stability and dispersion of nanoparticle is improved, the thermophysical properties can be modified and leads to drastic changes in hydraulic and thermal performance. Utilization of a MCHS does not only involve 1 unit of 1 cm by 1 cm, but many which translate into a high pumping power requirement.

6. Conclusion

We report in this study the optimization of a microchannel heat sink (MCHS) cooled with carbon nanotubes nanofluids flowing under laminar regime. This was done using multi-objective genetic algorithm (MOGA) to minimize simultaneously the thermal resistance and pressure drop of the MCHS. This optimization analysis was performed from viscosity and thermal conductivity values of carbon nanotubes nanofluids at 20°C that were experimentally obtained. Two types of CNT nanofluids were studied and mainly differs in types of surfactants used, lignin and sodium polycarboxylate, respectively. The effect of nanotube volume content and shape of channel section on the thermal and hydrodynamic performances was also investigated.

It was reported that nanofluids with lignin as surfactant produced a better thermal and hydrodynamic performance for the MCHS compared to the ones containing sodium polycarboxylate. This is attributed to higher viscosity of these later nanofluids as all other thermophysical properties are similar. As an example, a 29% and 28% increase in pressure drop is expected for sodium polycarboxylate based nanofluid at a volume fraction of 0.1% for a circular and square MCHS respectively. The pattern is observed at other volume fraction as well, even higher pressure drop with increasing volume fraction. Also, circular channel geometry presents a lower thermal resistance than square channel geometry. Thus, it is

imperative to properly determine the properties experimentally or use relevant models to predict the expected performance of nanofluid in flowing energy systems like microchannels before deciding on the nanofluids use in real applications.

Acknowledgements

The authors would like to thank the Universiti Teknologi Malaysia for the research grant Vot19H60 for the funding to do the research.

References

[1] Tuckerman D. B., Pease R. F. W. (1981). High-performance heat sinking for VLSI. IEEE Electron Device Letters, 5:126–9.

[2] M. B. Kleiner, S. A. Kuhn, K. Haberger, High performance forced air cooling scheme employing microchannel heat exchangers, IEEE Transactions on Components, Packaging, and Manufacturing Technology, Part A 20 (1995) 795-804.

[3] G. Gamrat, M. F. Marinet, D. Asendrych, Conduction and entrance effects on laminar liquid flow and heat transfer in rectangular microchannels, International Journal of Heat and Mass Transfer 48 (2005) 2943-2954.

[4] X. F. Peng, G. P. Peterson, B. X. Wang, Heat transfer characteristics of water flowing through microchannels, J. Exp. Heat transfer 7 (1995) 265-283.

[5] S. F. Choquette, M. Faghri, M. Charmchi, Y. Asako, Optimum design of microchannel heat sinks, ASME DSC 59 (1996) 115-126.

[6] W. Zhimin, C. K. Fah, Optimum thermal design of microchannel heat sinks, Proceeding of the 1997 1st Electronic Packaging Technology Conference, EPTC, Singapore, (1997) 123-129.

[7] A. Kosar, Effect of substrate thickness and material on heat transfer in microchannel heat sinks, International Journal of Thermal Sciences 49 (2010) 635-642.

[8] C. Perret, Ch. Schaeffer, J. Boussey, Microchannel integrated heat sinks in silicon technology, Proceedings of the 1998 IEEE Industry Applications Conference, USA, 2 (1998) 1051-1055.

[9] G. Hestroni, A. Mosyak, E. Pogerbnyak, L.P. Yarin, Heat transfer in microchannels: comparison of experiments with theory and numerical results, Int. J. Heat Mass Transf. 48 (2005) 5580-5601.

[10] J. McHale, S. V. Garimella, Heat transfer in trapezoidal microchannel of various aspect ratio, Int. J. Heat Mass Transfer 53 (19-20) (2010) 3683-3691.

[11] N. Ghazali-Mohd, J. T. Oh, B.C. Nguyen, K. I. Choi, , R. Ahmad, Comparison of the Optimized Thermal Performance of Square and Circular Ammonia-cooled Microchannel Heat Sink with Genetic Algorithm, Energy Conversion and Management 102 (2015) 59-65.

[12] A. Moradikazerouni, M. Afrand, J. Alsarraf, O. Mahian, S. Wongwises, M-D. Tran, Comparison of the effect of five different entrance channel shapes of a micro-channel heat sink in forced convection with application to cooling a supercomputer circuit board, Applied Thermal Engineering 150 (2019) 1078-1089.

[13] A. M. Adham, N. Mohd-Ghazali, R. Ahmad, Optimization of an ammonia-cooled rectangular microchannel heat sink using multi-objective non dominated sorting genetic algorithm (NSGA2), Heat and Mass Transfer, 48 (10) (2012) 1723-1733.

[14] T. C. Hung, W. M. Yan, X. D. Wang, C. Y. Chang, Heat transfer enhancement in microchannel heat sinks using nanofluids, Int. J. Heat Mass Transfer 55 (9-10) (2012) 2559-2570.

[15] S. Halelfadl, A. M. Adham, N. Mohd-Ghazali, T. Maré, P. Estellé, R. Ahmad, Optimization of thermal performances and pressure drop of rectangular microchannel heat sink using aqueous carbon nanotubes based nanofluid, Applied Thermal Engineering, 62(2) (2014), 492-499.

[16] A. M. Adham, N. Mohd-Ghazali, R. Ahmad, Thermal and hydrodynamic analysis of microchannel heat sinks: A review. Renewable and Sustainable Energy Reviews, 21 (2013), 614-622.

[17] Ping Li, Yaoyuan Luo, Di Zhang, Yonghui Xie, Flow and heat transfer characteristics and optimization study on the water-cooled microchannel heat sinks with dimple and pin-fin, International Journal of Heat and Mass Transfer, 119 (2018) 152-162.

[18] Y.F. Li, G.D. Xia, D.D. Ma, Y.T. Jia, J. Wang, Characteristics of laminar flow and heat transfer in microchannel heat sink with triangular cavities and rectangular ribs, International Journal of Heat and Mass Transfer, 98 (2016) 17-28.

[19] A. Moradikazerouni, M. Afrand, J. Alsarraf, S. Wongwises, A. Asadi, T. K. Nguyen, Investigation of a computer CPU heat sink under laminar forced convection using a structural stability method, International Journal of Heat and Mass Transfer 134 (2019) 1218-1226.

[20] R. Vinoth, D. Senthil Kumar, Channel cross section effect on heat transfer performance of oblique finned microchannel heat sink, International Communications in Heat and Mass Transfer, 87 (2017) 270-276.

[21] W. Duangthongsuk, S. Wongwises, An experimental investigation on the heat transfer and pressure drop characteristics of nanofluid flowing in microchannel with multiple zigzag flow channel structures, Exp; Thermal Fluid Sci. 87 (2017) 30-39.

[22] D. D. Vo, J. Alsarraf, A. Moradikazerouni, M. Afrand, H. Salehipour, C. Qi, Numerical investigation of γ-AlOOH nano-fluid convection performance in a wavy channel considering various shapes of nanoadditives, Powder Technology 345 (2019) 649-657.

[23] D. Byrne, R. A. Hart, A. K. Da Silva, Experimental thermal-hydraulic evaluation of CuO nanofluids in microchannels at various concentrations with and without suspension enhancers, Int. J. Heat Mass Transfer 55 (9-10) (2012) 2684-2691.

[24] A. M. Adham, N. Mohd-Ghazali, R. Ahmad, Optimization of nanofluid-cooled microchannel heat sink, Thermal Science, 20 (2016): 109-118.

[25] O. Mahian, L. Kolsi, M. Amani, P. Estellé, G. Ahmadi, C. Kleinstreuer, J. S. Marshall, M. Siavashi, R. A. Taylor, H. Niazmand, S. Wongwises, T. Hayat, A. Kolanjiyil, A. Kasaeian, I. Pop, Recent advances in modeling and simulation of nanofluid flows-Part I: Fundamentals and theory, Physics Reports 790 (2019) 1-48.

[26] T. Maré, P. Estellé, S. Halelfadl, N. Mohd-Ghazali, Consideration of Carbon Nanotube-based Nanofluid in Thermal Transfer, Jurnal Teknologi 78:8-4 (2016): 41-48.

[27] A.A. Arani, O.A. Akbari, M.R. Safaei, A.A.A.A Alrashed, G.R. Ahmadi, T.K. Nguyen, Heat transfer improvement of water/single-wall carbon nanotubes (SWCNT) nanofluid in a novel design of a truncated double-layered microchannel heat sink. Int. J. Heat Mass Transfer, 113 (2017) 780-795.

[28] M.M. Sarafraz, V. Nikkhaz, M. Nakhjavani, A. Arya, Fouling formation and thermal performance of aqueous carbon nanotubes nanofluid in a heat sink with rectangular microchannel, App. Thermal Eng. 123 (2017) 29-39.

[29] A. Abedin, A. Karimipour, D. Toghraie, The study of heat transfer and laminar flow of kerosene/multi-walled carbon nanotubes (MWCNTs) nanofluid in the microchannel heat sink with slip boundary condition, J. Thermal Ana. Cal. 131(2) (2018) 1553-1566.

[30] F. Su, X. Mu, Z. Lan. The effect of carbon nanotubes on the physical properties of a binary nanofluid. J. Taiwan Inst. Chem. Eng. 42 (2011) 252-257.

[31] S.M.S. Murshed, C.A. Nieto de Castro, Superior thermal features of carbon nanotubes-based nanofluids – A review, Renewable and Sustainable Energy Reviews, 37, 2014, 155-167.

[32] S.M.S. Murshed, P. Estellé, A state of the art review on viscosity of nanofluids, Renewable and Sustainable Energy Reviews, 76, 2017, 1134-1152.

[33] N. A. F. Nik-Mazlam, N. Mohd-Ghazali, T. Mare, P. Estellé, S. Halelfadl, Thermal and hydrodynamic performance of a microchannel heat sink cooled with carbon nanotubes nanofluid, Jurnal Teknologi (78:10-2) (2016) 69-77.

[34] A.A. Minea, P. Estellé, Numerical study on CNT nanofluids behavior in laminar pipe flow, Journal of Molecular Liquids 271 (2018) 281-289.

[35] P. Estellé, S. Halelfadl, T. Maré, Thermal conductivity of CNT water based nanofluids: Experimental trends and models overview, Journal of Thermal Engineering 1(2) (2015) 381-390.

[36] B.C. Pak, Y.I. Cho, Hydrodynamic and heat transfer study of dispersed fluids with sub - micron metallic particles. Exp. Heat Transfer. 1998 ;11: 151-170.

[37] H. O'Hanley, J. Buangiorno, T. McKrell, L.W. Hu, Measurement and model validation of nanofluid specific heat capacity with Differential Scanning Calorimetry. Adv Mech Eng 2012 181079.

[38] P. Estellé, S. Halelfadl, T. Maré, Thermophysical properties and heat transfer performance of carbon nanotubes water-based nanofluids, Journal of Thermal Analysis and Calorimetry, 127 (2017) 2075-2081.

[39] P. Estellé, S. Halelfadl, T. Maré, Lignin as dispersant for water-based carbon nanotube nanofluids: Impact on viscosity and thermal conductivity, International Communications in Heat and Mass Transfer 57 (2014) 8-12

[40] Halelfadl S., Caractérisation des propriétés thermo-physiques et d'échanges de chaleur des nanofluides à base de nanotubes de carbone, PhD Thesis, Insa Rennes, December 2014.

Nomenclature

L	-	Length
W	-	Width
t	-	Substrate thickness
H_c	-	Channel height
W_c	-	Channel width
W_w	-	Wall width
R_{cond}	-	Conduction thermal resistance
R_{cap}	-	Capacitive thermal resistance
R_{conv}	-	Convective thermal resistance
R_{total}	-	Total thermal resistance
G	-	coolant flow rate
k_s	-	Thermal conductivity of substrate
Nu	-	Nusselt number
Re	-	Reynolds number
k	-	Thermal conductivity of nanofluid
ρ	-	Density of nanofluid
μ	-	Viscosity of nanofluid
c_p	-	Specific heat capacity of nanofluid
α	-	Hydraulic diameter
β	-	Wall width to channel width ratio

ΔP	-	Pressure drop